available at www.sciencedirect.com

www.elsevier.com/locate/matchar

Use of time history speckle pattern and pulsed photoacoustic techniques to detect the self-accommodating transformation in a Cu–Al–Ni shape memory alloy

F.M. Sánchez-Arévalo[a,*], W. Aldama-Reyna[b], A.G. Lara-Rodriguez[c], T. García-Fernández[d], G. Pulos[c], M. Trivi[e], M. Villagran-Muniz[a]

[a]CCADET — Universidad Nacional Autónoma de México, A.P. 70-186, México D.F., C.P. 04510, México
[b]Departamento Académico de Física, Universidad Nacional de Trujillo, Trujillo, Perú
[c]Instituto de Investigaciones en Materiales, Universidad Nacional Autónoma de México, México
[d]Universidad Autónoma de la Ciudad de México (UACM), Prolongación San Isidro 151, Col. San Lorenzo Tezonco, México DF, C.P. 09790, México
[e]Centro de Investigaciones Opticas, Universidad de la Plata, Argentina

ARTICLE DATA

Article history:
Received 22 July 2009
Received in revised form
6 February 2010
Accepted 14 February 2010

Keywords:
Digital speckle pattern correlation
Time history speckle pattern
Photoacoustics
Martensitic transformation
Shape memory alloy
CuAlNi

ABSTRACT

Continuous and pulsed electromagnetic radiation was used to detect the self-accommodation mechanism on a polycrystalline Cu–13.83 wt.%Al–2.34 wt.%Ni shape memory alloy. Rectangular samples of this alloy were mechanically polished to observe the austenite and martensite phases. The samples were cooled in liquid nitrogen prior to the experiments to obtain the martensite phase. Using a dynamic speckle technique with a continuous wave laser we obtained the time history of the speckle pattern image and monitored the surface changes caused by the self-accommodation mechanism during the inverse (martensitic to austenitic) transformation. Using a photoacoustic technique based on a pulsed laser source it was also possible to detect the self-accommodation phenomena in a bulk sample. For comparison purposes, we used differential scanning calorimetry (DSC) to detect the critical temperatures of transformation and use these as reference to evaluate the performance of the optical and photoacoustical techniques. In all cases, the same range of temperature was obtained during the inverse transformation. From these results, we conclude that time history speckle pattern (THSP) and pulsed photoacoustic are complementary techniques; they are non-destructive and useful to detect surface and bulk martensitic transformation induced by a temperature change.

1. Introduction

Recently, the scientific and technologic community has been interested in the study of thermomechanical behavior observed in some "exotic materials" like shape memory alloys (SMAs). These materials present some associated effects like single or double shape memory effects [1] or superelastic effect [2]. These are due to a martensitic transformation, which is a first-order displacive process, where a body center cubic parent phase (austenitic phase) transforms by a shearing mechanism into a (monoclinic or orthorhombic) martensitic phase. This displacive process in SMAs is a crystalline phase change which can be driven either by a temperature change, stress or both. When the martensitic transformation is driven by a temperature change,

* *Corresponding author*. Tel./fax: +52 55 5622 4602.
E-mail address: fsanchez@iim.unam.mx (F.M. Sánchez-Arévalo).

1044-5803/$ – see front matter © 2010 Elsevier Inc. All rights reserved.
doi:10.1016/j.matchar.2010.02.008

four critical temperatures can be identified: M_s and M_f that correspond to the start and finish of the direct transformation (austenite to martensite phase) while A_s and A_f correspond to the start and finish of the inverse transformation (martensite to austenite phase). As a result of the martensitic transformation, the mechanical behavior of the material is modified.

When the martensitic transformation is driven by a temperature change, a self-accommodating mechanism takes place in the solid phase change. In this case the martensitic plates grow in all possible directions making all 24 possible variants appear in the material [3,4]. These variants cause surface and bulk changes on the microstructure of the material that can be detected by different techniques such as differential scanning calorimetry (DSC), electrical extensometry, metallographic analysis or mechanical spectroscopy and others [5–7]. The use of these techniques to detect the martensitic transformation is not always convenient due to their invasive or destructive character or the size of the samples. In some cases, a non-destructive technique is required to detect this phase transformation in order to predict the mechanical behavior of the material as was reported previously [6,7]. The combination of conventional experimental techniques to determine the mechanical behavior of materials has afforded new alternatives to get a better understanding of materials [8].

Considerable efforts have been made to understand the complex behavior of SMAs, mainly because their properties will eventually lead to replace conventional materials with these alloys. To the author's knowledge, the martensitic transformation in Cu–13.83 wt.%Al–2.34 wt.%Ni induced by a temperature change using time history speckle pattern (THSP) and pulsed photoacoustic (PA) techniques has not been studied until now. In this paper, we report on the use of non-destructive techniques for studying self-accommodating transformation of the CuAlNi shape memory alloy. Time history speckle pattern and pulsed photoacoustic together with image analysis are used to evaluate the critical temperatures of the transformation, and these are compared with those obtained by conventional DSC technique.

2. Dynamic Speckle

The speckle effect is a feature resulting from the interaction of coherent illumination with an optically-rough surface. This effect is described as the interference of mutually coherent waves having accidentally varying phases. The result of such interference is the distribution of maxima and minima of light intensity with random phase and the individual intensity peaks representing the bright or dark spots are known as speckles. A group of these speckles is called the speckle pattern [9] and, when a sample is illuminated with a laser, the speckle pattern is useful to monitor the changes in the surface due to displacement, strain or biological activity [10–15]. One possible approach to analyze the evolution of dynamic speckle is by means of the time history speckle pattern (THSP). The THSP is based on reconstructing an image using a sequence of speckle pattern variations. A series of images is acquired and, by selecting the same column of each image, the speckle variation on this particular column can thus be estimated. As depicted in Fig. 1, the THSP represents the evolution in time of the speckle pattern constructed through a sequence of images. Therefore, the changes on the surface can be monitored upon correlating the changes registered along the horizontal direction of the THSP image [16,17].

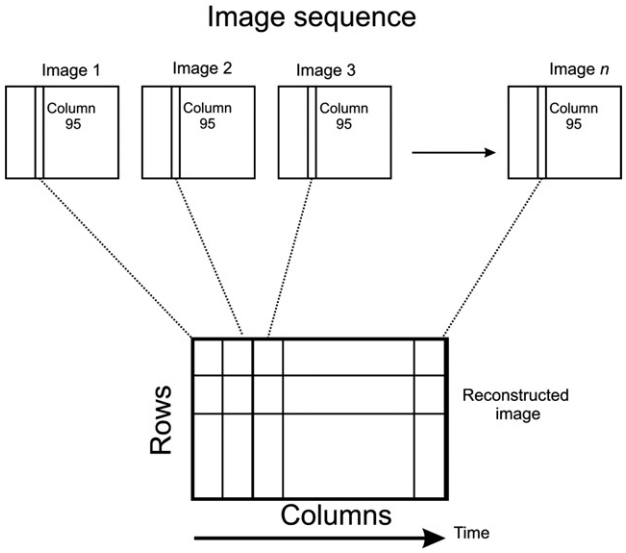

Fig. 1 – Reconstruction of the THSP image.

3. Photoacuostics

The photoacoustic effect (PA effect), related to the generation of acoustic waves in a medium after interaction with modulated or pulsed laser radiation, has been proven useful to detect thermoelastic parameters such as thermal expansion, sound velocity, heat capacity, etc. [18–20]. Photoacoustic techniques using lasers (pulsed electromagnetic radiation) and piezoelectric transducers have also become an interesting means to characterize bulk behavior in materials [18–24]. In the thermoelastic regime,[1] the acoustic waves generated with laser pulses are detected with a piezoelectric transducer.

The photoacoustic signal is represented by the function $PA(t,T_i)$, where t represents the time and T is a parameter indicating the physical parameter of interest (e.g., strain, temperature, etc.). In our case, T represents the temperature and i denotes the incremental step in temperature [24]. The $PA(t,T_i)$ function is obtained experimentally and it can be used for further mathematical analysis to provide important physical information related to features of the sample.

The direct coupling method is commonly used to detect structural change; this is based on the following considerations: the acoustic wave is related to the thermal expansion ΔV_{th} of the irradiated volume V_o. In this case ΔV_{th} can be written as $\Delta V_{th}=(\beta/C_p\rho)H$, where β is the volume expansion coefficient of compressibility, C_p is the specific heat at constant pressure, ρ is the density and H is the heat deposited in the volume V_o. This expansion creates a pressure wave which travels outwards at the velocity of sound and the electrical signal generated in the transducer is proportional to pressure.

[1] When no ablation occurs.

The temporal profile of the acoustic pressure depends on the spatial properties and microscopic characteristics of those regions where the ultrasonic wave interacts with the sample. In this case, since the martensitic and austenitic phases have different Young's moduli and densities, the phases have different wave speeds and the photoacoustic signal can be used to monitor the phase transformation.

4. Experimental Details

To obtain the shape memory alloy an Ar-controlled atmosphere induction furnace (Leybold-Heraeus) was used. In addition, the casting was subjected to a homogenization heat treatment during 96 h at 900 °C. Then the ingot was hot-rolled to obtain thin sheets which were cut in small rectangular slices with dimensions of 35, 6 and 0.6 mm in length, width, thickness respectively. After the hot-rolled process a quantitative element concentration analysis was carried out by an energy-dispersive X-ray spectrometer (EDS)—Oxford PentaFet—mounted in a LEICA Stereoscan 440 microscope. Subsequently, the DSC analysis was done to detect the critical temperatures of the alloy; finally, the samples were mechanically polished and no chemical agent was needed to observe the phases in the material.

5. Optical Experiment

The samples were cooled down using liquid nitrogen and then allowed to warm up to −10 °C prior to the start of the experiment to transform the sample into martensite. Afterwards, the samples were placed on a heater, which was regulated by an INSTEC STC200 controller; subsequently, the temperature was increased from −10 to 70 °C. During the heating, images of the sample surface were acquired by a CCD camera (640×480 pixels) coupled to a modular microscope as shown in Fig. 2. The time, temperature and images were acquired by an 8331, 6281 and 1409 National Instruments boards mounted in a PXI-1002 chassis. A LabVIEW virtual instrument was used to synchronize the data acquisition with the PC.

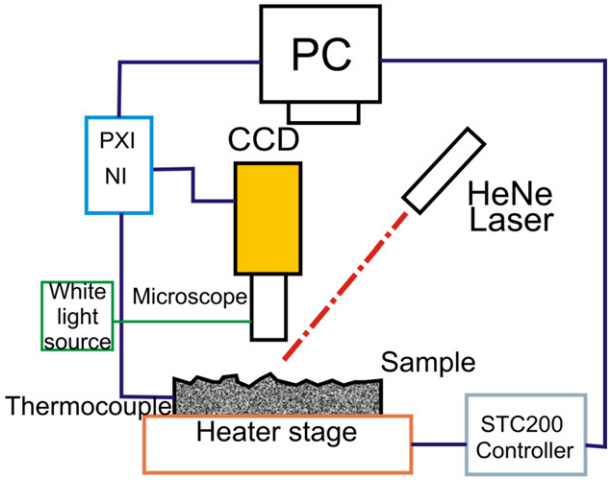

Fig. 2 – Experimental setup to observe the dynamic speckle.

Two kinds of illumination systems were used to observe the CuAlNi surface. The first one was a 150 W quartz halogen white light source and the second one was a Melles Griot HeNe laser (632 nm, 20 mW). The white light was used to observe a typical metallographic image where the disappearance of martensitic plates was registered by the camera after heating. The continuous wave (CW) laser illumination was used to produce the speckle pattern on the sample surface.

With the image sequence, digital image analysis was used to observe the phase change with white light and laser as a function of temperature changes. Using white light, it was possible to qualitatively determine the phase change while using laser illumination a quantitative determination of phase transformation has been measured by determining the speckle activity of the THSP image. To quantify the speckle activity of this image, the cross-correlation function was used; in this case the two input signals were the gray scale intensities of the i and i_{+1} columns of the THSP image. The normalized correlation index between pairs of columns of the THSP image was calculated using the *xcorr(x,y,'coeff')* function of MATLAB™.

6. Photoacoustic Experiment

The experimental setup for the photoacoustic measurement of phase transition induced by temperature is shown in Fig. 3. Pulses of 0.9 mJ from the second harmonic ($\lambda = 532$ nm) of a Nd:YAG laser (Continuum, model Surelite I, 10 Hz, 5 ns) were used. To measure in real time the energy variations of the laser, a beam splitter and power energy meter (Scientech 365) were used; additionally, an iris diaphragm with a diameter of 2 mm was used to collimate the beam.

An electric tubular furnace (Thermolyne 21100) was used to heat a rectangular slice of CuAlNi from 20 °C to 70 °C with a heating rate of 1 °C/min. The sample was centered in the furnace and it was glued to a quartz bar[2] to transmit the ultrasonic signal outside the furnace; water was circulated around the external end of the bar to avoid heating the PZT sensor. The cylindrical PZT transducer has a resonance frequency at 136 kHz and the signals without amplification were recorded in a Tektronix TDS5054B digital oscilloscope. Triggering was obtained from a photodiode that registered the scattered light and the acquired signals were post-processed in MATLAB™.

7. Results

After the melting, the homogenization and the hot-rolling processes thin slides of Cu–13.83 wt.%Al–2.34 wt.%Ni alloy were obtained. According to this alloy composition and the empirical equation, $M_s(°C) = 2433 - 169.6(wt.\%Ni) - 19.1(wt.\%Al)$, the M_s temperature must be around 37 °C [25]. From the DSC[3] results it can be observed that the M_s temperature was around 32 °C. This result showed an acceptable agreement between the calculated and measured M_s temperatures.

[2] The diameter and length of the bar were 5 mm and 29 cm respectively.

[3] The heat flow as a function of temperature is determined [26].

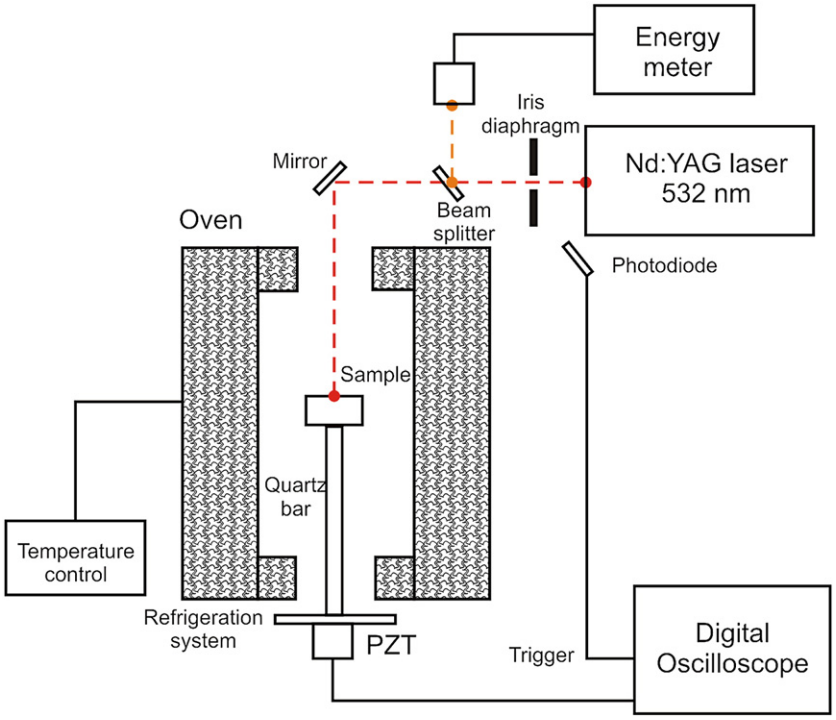

Fig. 3 – Photoacoustical experiment setup.

The critical temperatures are shown in Fig. 4, where M_s=32 °C, M_f=8 °C, A_s=46 °C and A_f=59 °C. In this figure the highest peaks during cooling (exothermic reaction; where the heat flow increased appreciably) and heating (endothermic reaction; where the heat flow decreased appreciably) are also indicated; their temperatures were M_m=26 °C and A_m=53 °C respectively. The critical temperatures obtained by DSC confirmed that the CuAlNi alloy has the shape memory effect in the mentioned range.

The CuAlNi alloy was observed by optical microscopy at two different temperatures. Metallographic images for each phase were obtained using white light; the martensitic and austenitic phases are shown in Fig. 5. Fig. 5a, where the probe temperature was above A_f, shows a plain surface corresponding to an austenitic phase around 70 °C. In this case the austenitic phase predominates; nevertheless three very small needles of martensitic phase were present. Fig. 5b, where the probe temperature was under M_f, shows the martensitic phase around −10 °C. Here martensitic plates can be observed perfectly with a width between 100 and 250 μm. The growth of martensitic plates changed the roughness of the sample and therefore the optical texture that was registered by the CCD.

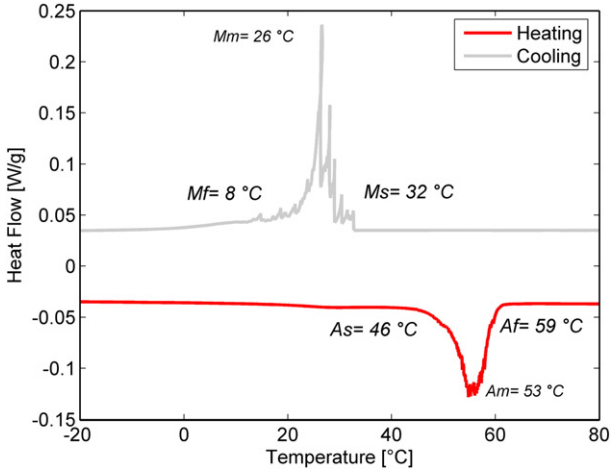

Fig. 4 – Critical temperatures obtained by DSC.

The roughness of the sample allowed observing the speckle effect when the coherent light of the He–Ne laser illuminated the sample. This pattern remained without significant changes until the martensitic plates began to appear. The pattern was captured by the CCD camera and two representative patterns are shown in Fig. 6. Fig. 6a shows a pattern that corresponds to austenitic phase. This image shows a speckle pattern with a regular distribution in the gray scale. Fig. 6b represents the pattern obtained when the sample has already transformed to the martensitic phase; in this pattern some regions with medium size white dots can be observed causing some irregularities in the gray scale distribution. These dots indicate that the martensitic phase is now present in the sample. The change in phase is more evident in Fig. 5b where the same region was observed using white light. The two kinds of illumination complement each other since the phase change can be easily detected with white light and the speckle patterns from the laser illumination are more amenable to analysis.

From the sequence of this kind of images, during the heating of the sample (−10 to 70 °C), the THSP image, as described in the optical experiment section, was obtained. In Fig. 7 the THSP image for one column is shown. This image represents the evolution of one column in the speckle pattern during the experiment; in this case, the activity on the surface is observed as the pixel intensity changes along the horizontal direction of the THSP image. The

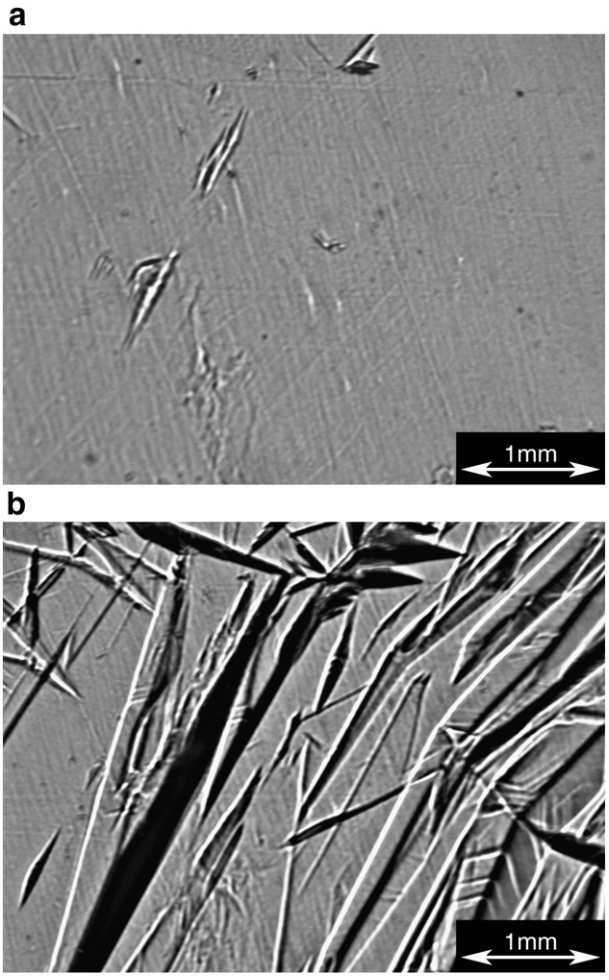

Fig. 5 – Metallographic observation of phase transition of CuAlNi shape memory alloy using white light source. a) Austenitic phase [70 °C]. b) Martensitic phase [−10 °C].

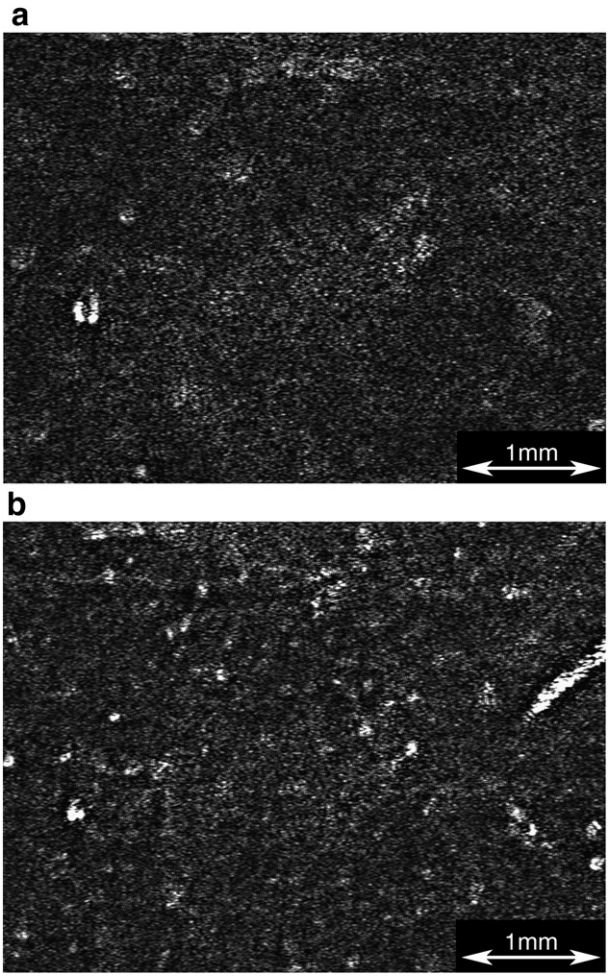

Fig. 6 – Speckle images of phase transition of CuAlNi shape memory alloy using laser illumination. a) Digital speckle pattern in austenitic phase. b) Digital speckle pattern in martensitic phase.

temperatures[4] when there is more activity on the surface occur in the middle of the THSP; in contrast, times with the lowest activity on the surface occur at the left and right edges. In these regions black and white straight lines can be observed as a result of the reduced activity. The martensitic transformation as a function of temperature changes the topography of the surfaces, which in turn produces changes in the speckle pattern. Thus, when the inverse martensitic transformation occurred on the sample's surface, the results can be observed from the THSP image; the critical points—beginning and ending of the transformation—can qualitatively be obtained from this image.

In order to get a quantitative result, a cross-correlation function was applied to compare the columns i *vs* i_{+1} of the THSP image as intensity profiles. The result of this analysis was calculated using MATLAB™ and the resulting correlation coefficient indicates how similar or different the compared columns are. The values of the correlation coefficient range from 1 for identical intensity profiles to 0 representing complete different intensity profiles. The calculated correlation coefficient as a function of temperature is the white line in Fig. 7. In this line three regions can be observed where the activity on the surface changed the speckle pattern and obviously the correlation coefficient as well. These regions represent the critical temperatures associated

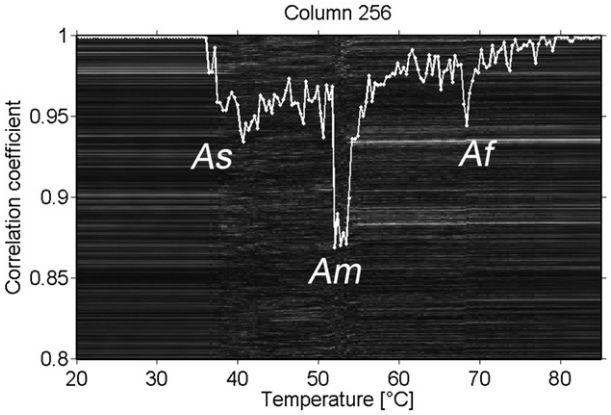

Fig. 7 – Determination of critical temperatures during the inverse transformation using continuous laser radiation (column 256).

[4] Or equivalently, the time since a heating ramp was prescribed.

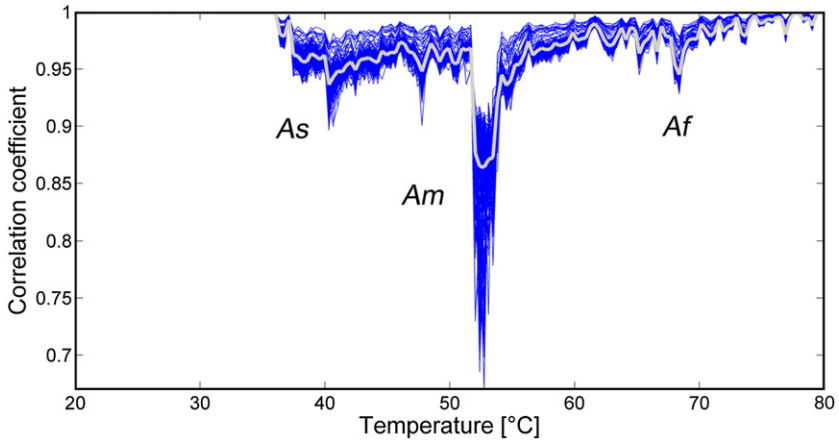

Fig. 8 – Average of the correlation coefficient during the inverse martensitic transformation obtained by dynamic speckle.

to the inverse martensitic transformation of the CuAlNi. Using this analysis the calculated temperatures were around A_s=42 °C, A_m=53 °C, A_f=66 °C; where A_m represents the maximum surface activity (smallest correlation coefficient) in the inverse transformation.

Taking all the columns of the image and doing the same procedure, the average of the correlation coefficient was obtained. This coefficient as a function of temperature (gray line) together with the individual traces is shown in Fig. 8. It is clear that the (average) correlation coefficient is not significantly different from the individual traces and can be used to obtain the critical temperatures.

From the photoacoustic experiment, three acoustic signals—obtained directly from the oscilloscope and without amplification—are shown at different temperatures in Fig. 9. The continuous black line represents a signal that corresponds to a temperature around 30 °C. It is clear that this signal begins with negative amplitude values. When the temperature is increased above A_s there are notable changes in the signal: the most interesting one occurs when the acoustic signal suffered a sign change at A_m=55 °C. Now the signal begins with positive values in its amplitude as can be observed from the dark dashed line. This is because the ratio ($\beta/C_p\rho$) changes from negative to positive when the inverse transformation takes place (around 54 °C). In the same figure another positive signal is shown at a higher temperature than A_f; in this cases, the signal stays positive (light dashed line). In addition, a change in sound velocity through the material was observed. In the martensitic phase the signal begins earlier than in the austenitic phase; this shows that the sound velocity is higher in the first one and reflects the phase change that has occurred in the material. In this case the pulsed laser interaction with the crystalline structure of the material gives different responses for the different phases. After the observed first peaks in Fig. 9, rebounds were also detected; they correspond to reflections of the acoustic wave in different contact surfaces between the couplings of sample, quartz rod and transducer [27].

In Fig. 10, the correlation coefficient for consecutive photoacoustic signals is shown. From this analysis, the temperatures of the bulk phase transition can be detected. This photoacoustical

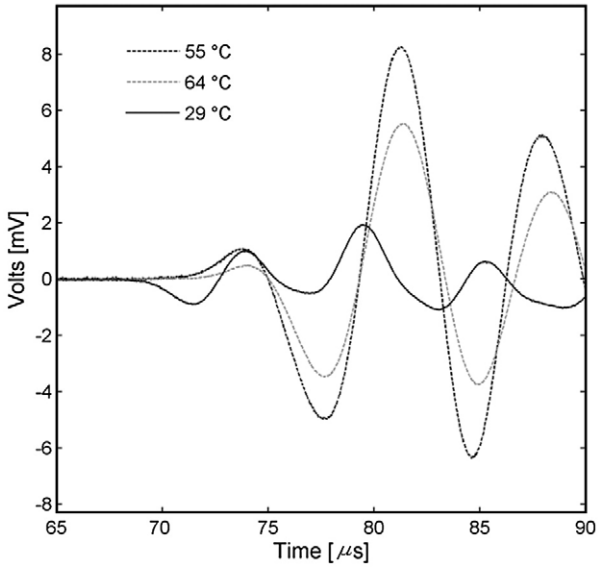

Fig. 9 – Photoacoustic signals at different temperatures.

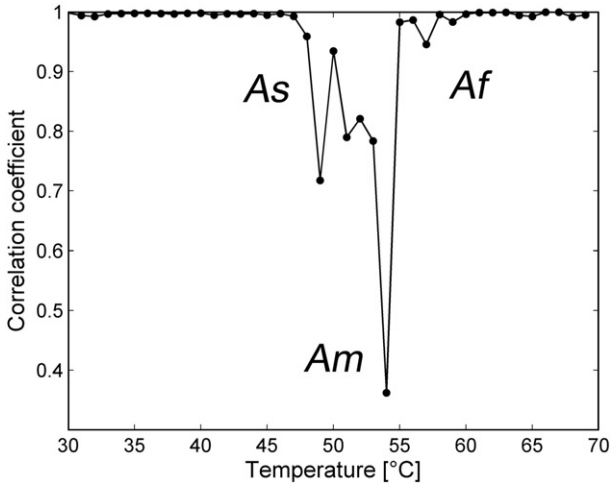

Fig. 10 – Correlation coefficient determined by photoacoustic measurements.

Table 1 – Temperatures of transformation.

Temperatures [°C]	Technique		
	DSC	THSP	PA
A_s	46	42	47
A_m	53	53	54
A_f	59	66	60

result gives the critical temperatures around the following values: A_s=47 °C, A_m=54 °C, A_f=60 °C which are in agreement with those obtained by THSP and DSC. Therefore both techniques, THSP and photoacoustic, can be used to monitor the martensitic transformation induced by temperature.

The results are summarized in Table 1.

In this table, it can be observed that there is an agreement between A_s, A_f and A_m using the three different techniques (DSC, THSP and PA). Nevertheless there is a small deviation in the A_f temperature obtained by the THSP technique. This variation may be due to a gradient of temperature of the air between the sample and the lenses of the camera. This gradient may affect the stability of the speckle pattern.

8. Conclusion

The results of this work show that time history speckle pattern (THSP) and pulsed photoacoustics are useful techniques to detect the inverse martensitic transformation. During the self-accommodation phenomena, it was possible to detect the superficial and bulk changes in this material using these techniques. Both techniques allowed us to determine the transformation temperature range, which is in agreement with the one obtained from a standard technique such as DSC.

The techniques present a powerful alternative to monitor the martensitic transformation in some mechanical elements typically used as damping elements.

Acknowledgements

This work was developed with financial support from Instituto de Ciencia y Tecnología del Distrito Federal (ICyTDF), and the DGAPA-UNAM program through grants IN114009. UNAM CTIC-DGAPA provided a postdoctoral fellowship for F.M.S.A. The authors are grateful to Esteban Fregoso and Omar Novelo for their technical support and to Juan Hernández-Cordero and Rosalba Castañeda for their comments to this work.

REFERENCES

[1] Patoor E, Berveiller M. Les alliages à mémoire de forme. Hermes, PARIS: Technologies de pointe; 1990.
[2] Wayman CM, Duerig TM. An introduction to martensite and shape memory. Engineering aspects of shape memory alloys. London: Butterworth-Heinemann; 1990. p. 3–20.
[3] Yang JH, Wayman CM. Self-accommodation and shape memory mechanism of ε-martensite I. Experimental observations. Mater Charact 1992;28:23–35.
[4] Yang JH, Wayman CM. Self-accommodation and shape memory mechanism of ε-martensite II. Theoretical considerations. Mater Charact 1992;28:37–47.
[5] Lambri OA, Pérez-Landazábal JI, Cuello GJ, Cano JA, Recarte V, Siemers C, et al. Mechanical spectroscopy in Fe–Al–Si alloys at elevated temperatures. J Alloys Compd 2009;468:96–102.
[6] Sánchez-Arévalo FM, Pulos G. Use of digital image correlation to determine the mechanical behavior of materials. Mater Charact 2008;59:1572–9.
[7] Sánchez-Arévalo FM, García Fernández T, Pulos G, Villagran-Muniz M. Use of digital speckle pattern correlation to strain measurements in a CuAlBe shape memory alloy. Mater Charact 2009;60:775–82.
[8] Field JE, Walley SM, Proud WG, Goldrein HT, Siviour CR. Review of experimental techniques for high rate deformation and shock studies. Int J Impact Eng 2004;30:725–75.
[9] Shchepinov VP, Pisarev VS, Novikov SE, Balalov VV, Odinstev OI, Bondarenko MM. Strain and stress analysis by holographic and speckle interferometry. West Sussex, England: John Wiley & Sons Ltd.; 1996. 483.
[10] Braga Jr RA, Dal Fabbro IM, Borem FM, Rabelo G, Arizaga R, Rabal HJ, et al. Assessment of seed viability by laser speckle techniques. Biosyst Eng 2003;86(3):287–94.
[11] Braga Jr RA, Rabelo GF, Granato LR, Santos EF, Machado JC, Arizaga R, et al. Detection of fungi beans by the laser biospeckle technique. Biosyst Eng 2005;91(4):465–9.
[12] Passoni I, Dai Pra A, Rabal H, Trivi M, Arizaga R. Dynamic speckle processing using wavelets based entropy. Opt Commun 2005;246:219–28.
[13] Tebaldi M, Ángel L, Bolognini N, Trivi M. Speckle interferometric technique to assess soap films. Opt Commun 2004;229:29–37.
[14] Braga Jr RA, Olivera B, Rabelo G, Marques R, Machado A, Cap N, et al. Reliability of biospeckle image analysis. Opt Lasers Eng 2007;45:390–5.
[15] Jiang Huifeng, Zhang Qingchuan, Chen Xuedong, Chen Zhongjia, Jiang Zhenyu. Three types of Portevin-Le Chatelier effects: experiment and modeling. Acta Mater 2007;55: 2219–28.
[16] Arizaga R, Trivi M, Rabal H. Opt Laser Technol 1999;31:163.
[17] Federico A, Kaufmann GH, Galizzi GE, Rabal H, Trivi M, Arizaga R. Simulation of dynamic speckle sequences and its applications to the analysis of transient processes. Opt Commun 2006;260:493–9.
[18] Etxebarria J, Uriarte S, Fernandez J, Tello MJ, Gomez-Cuevas A. J Phys C: Solid State Phys 1984;17:6601–10.
[19] Tocho JO, Cusso F, Ramirez R, Gonzalo JA. Appl Phys Lett 1991;59:1684.
[20] Castañeda-Guzman R, Villagran Muniz M, Saniger Blesa J, Perez O. Appl Phys Lett 1998;73(5):623–5.
[21] Castañeda-Guzman R, Villagran Muniz M, Saniger Blesa J, Perez O. Bol Soc Esp Cer Vidrio 1999;38(5):439–42.
[22] Castañeda-Guzman R, Perez Ruiz SJ, Villagran-Muniz M, Saniger Blesa J. Anal Sci 2001;17:s122–5.
[23] Pineda Flores JL, Castañeda-Guzman R, Villagran-Muniz M, Huanosta-Tera A. Appl Phys Lett 2001;79(8):1166–8.
[24] Huanosta-Tera A, Castañeda-Guzman R, Pineda-Flores JL. Mater Res Bull 2003;38:1073–9.
[25] Recarte V, Pérez-Sáez RB, Bocanegra EH, Nó ML, San Juan J. Influence of Al and Ni concentration on the martensitica transformation in Cu–Al–Ni Shape memory alloys. Metall Mater Trans A-Phys Metall Mater Sci 2002;33A:2581–91.
[26] Mackenzie RC. Differential thermal analysis. London NW1: Academic Press; 1972.
[27] Villagrán-Muniz M, García-Segundo C, Ranea-Sandoval HF, Bilmes GM. Rev Sci Instrum 1995;66:3500.